Estimation of local Mach number in compressible flows of dense organic vapors using Gabor filters and Radon transforms for the post-processing of schlieren images

Michelis, Theodoros; Head, Adam; Colonna, Piero

DOI
10.1007/s00348-024-03925-7

Publication date
2024

Document Version
Final published version

Published in
Experiments in Fluids

Citation (APA)
Michelis, T., Head, A., & Colonna, P. (2024). Estimation of local Mach number in compressible flows of dense organic vapors using Gabor filters and Radon transforms for the post-processing of schlieren images. *Experiments in Fluids*, *65*(12), Article 185. https://doi.org/10.1007/s00348-024-03925-7

Experiments in Fluids (2024) 65:185
https://doi.org/10.1007/s00348-024-03925-7

RESEARCH ARTICLE

Estimation of local Mach number in compressible flows of dense organic vapors using Gabor filters and Radon transforms for the post-processing of schlieren images

Theodoros Michelis[1] · **Adam Head**[1] · **Piero Colonna**[2]

Received: 19 August 2024 / Revised: 1 October 2024 / Accepted: 6 November 2024 / Published online: 28 November 2024

Abstract
Images of compressible flows can be post-processed with digital imaging techniques to obtain accurate quantitative information about variables characterizing the flow. For example, the local flow Mach number can be obtained from the angle of Mach lines visualized with the schlieren method. These techniques were recently applied to supersonic flows of dense organic vapors, with the objective of obtaining accurate data to validate theory and CFD codes. Non-ideal compressible fluid dynamics (NICFD) is concerned with these flows, for which therefore the thermodynamic properties of the fluid can be modeled only with equations that are more complex than the ideal gas relations. NICFD flows are relevant, e.g., for applications in the power and chemical industry. However, currently employed image post-processing techniques used to obtain the local Mach number or shock wave angle from schlieren images, like the Hough transform, suffer from few drawbacks, namely a long computational time to obtain the relevant quantities and improvable accuracy. The investigation reported here concerns the application of known digital image processing methods to schlieren images, in this case Gabor filters and Radon transforms, to obtain the local Mach number and the shockwave angle of flows in NICFD conditions. The selected test case is the supersonic expansion of the dense vapor of hexamethyldisiloxane flowing through the nozzle test section of the ORCHID facility in operation at the Propulsion and Power laboratory of Delft University of Technology. The investigated digital image processing techniques provide values of the local Mach number with comparable uncertainty (within 5%) as the Hough transform approach. Moreover, Mach line orientations are computed for the whole field of view, together with Mach line wavelength. It was also proven that these methods are suitable for discerning Mach line orientation even in the case of very complex flow fields, with coexisting Mach waves and shock waves.

1 Introduction

If flows are highly compressible, e.g., if the flow is highly supersonic, flow features directly related to compressibility effects become more evident. Examples include acoustic waves, Mach lines, oblique shockwaves and expansion fans. These flow features are typically visualized by means of the well-known schlieren technique, which provides an image of the flow field whereby light intensity directly relates to the density gradient. Quantitative information retrievable from schlieren images is often limited to the identification of the local angle of such flow features, which can be subsequently used to infer other quantities of interest such as the Mach number (e.g., Head et al. 2023). In flows for which the total enthalpy is constant such as in ideal gas dynamics, it is often possible to obtain the velocity field with Particle Image Velocimetry (PIV), whereby the Mach number and flow direction can be directly estimated via the velocity vector (e.g., D' Aguanno et al. 2022). However, in conditions for which the total enthalpy is variable across the domain, such as for expanding vapors of dense organic fluids (Guardone et al. 2024), measurement methods of two-dimensional velocity fields are not readily available (Michelis et al. 2024). Hence, the possibility of precisely identifying the angle of flow features from schlieren images becomes particularly relevant in order to estimate the Mach number distribution.

✉ Theodoros Michelis
t.michelis@tudelft.nl

[1] Flow Physics and Technology, Aerospace Engineering, Delft University of Technology, Delft, The Netherlands

[2] Propulsion and Power, Aerospace Engineering, Aerospace Engineering, Delft University of Technology, Delft, The Netherlands

Several techniques to measure the orientation of supersonic flow features have been developed over the last decades (Randen and Husøy 1999). Initially, researchers employed a simple protractor to estimate angles of flow features from flow field photographs. With the emergence of high-performance computing and digital imaging techniques, a variety of specific algorithms often relying on edge detection methods were developed and successfully used. These include, for example, the use of the Hough transform to detect lines and curves in grayscale images (Duda and Hart 1972; Lo and Tsai 1995) by linearly parametrizing the images to obtain families of concurrent lines. The group of pixels that belong to each visualized line (Mach line or shock) can be subsequently used to calculate the corresponding angle (e.g., Spinelli et al. 2018; Head et al. 2023). However, these techniques suffer from several limitations such as the sensitivity of edge detection to local light intensity and to insufficient signal-to-noise ratio, as well as to excessive line thickness. Most importantly, the robustness of these methods drastically decreases if variable angles and curved lines are considered.

Gabor filtering is a powerful mathematical and computational technique used in signal processing and image analysis. It is based on the Gabor wavelet, a complex-valued function which modulates sinusoidal waves with a Gaussian envelope. This unique combination allows to use Gabor filters to represent and analyze both the frequency and the spatial localization of features within signals or images. Originally inspired by the ability of the human visual system to perceive textures at various scales and orientations (Field et al. 1993), Gabor filters are widely employed in diverse fields such as computer vision, neuroimaging, and pattern recognition (e.g., Arrospide and Salgado 2013). These filters are characterized by their ability to efficiently capture essential information from input data, making them indispensable in applications like edge detection, texture segmentation, and feature extraction (e.g., Jain and Farrokhnia 1991). Gabor filtering is, therefore, also applicable to the identification of supersonic flow features in schlieren images.

Another image analysis technique often adopted for the treatment of medical images (e.g., Tam et al. 1998) and relying on the discrete Radon transform (Beylkin 1987) feature characteristics that make it suitable for post-processing schlieren images of supersonic flows. The discrete Radon transform involves the integration of a function, typically representing image light intensity, along various straight-line trajectories at diverse angles. These integrals, denoted as projections, encapsulate pertinent information regarding the internal structure of the subject under examination. Through analysis of these projections, a comprehensive two-dimensional representation is constructed, elucidating the geometric attributes of the object and their orientation. In the field of compressible fluid mechanics and acoustic imaging, the Radon transform analysis method has proven invaluable for quantitatively determining the local shock propagation angle of supersonic jet outlets (Murray and Lyons 2016; Canchero et al. 2016). Although the Radon transform methodology is a simple and robust method to obtain the local orientation of features, it can be extended to provide spatial wavelength, if the features are periodic in space. The operation must be performed within interrogation windows, potentially lowering the achievable spatial resolution, unless overlapping of interrogation windows is applied.

This article reports an investigation about the suitability of methods based on the Gabor filter and on the Radon transform to quantitatively determine the orientation and wavelength of flow features due to compressibility, such as Mach lines and shock waves. For the purpose of this investigation, a dataset of schlieren images of supersonic flows of a dense organic vapor expanded in a de Laval nozzle was analyzed. The aim is to quantify the Mach number via the Mach wave orientation at the center of the nozzle. Two-dimensional fields of both orientation and wavelength of the evident flow features were obtained, pivoting on the inherent capabilities of the proposed techniques to detect spatial orientation and frequency in a single operation. In addition, a means of statistically estimating the associated uncertainties is proposed, considering the second statistical moment of the Gabor filtering convolution coefficient and the Radon transform amplitude.

2 Experimental dataset

The dataset used to illustrate the application of the image processing methods pertains to the schlieren image of a supersonic dense organic vapor flowing through the nozzle test section of the ORCHID facility in operation at the Propulsion and Power laboratory of Delft University of Technology (Head 2021). The thermodynamic state of the working fluid, hexamethyldisiloxane (MM), at the inlet of the test section is that defined by a temperature of 253 °C and absolute pressure of 18.4 bar. A metallic wedge whose function is to generate oblique shockwaves is located at the outlet of the nozzle test section. A raw schlieren realization is shown in Fig. 1a, where weak Mach waves can be observed throughout the field of view. The Mach lines (weak acoustic waves) are not intentionally produced by any periodic surface roughness. Instead, they align with the characteristic lines of the nozzle and arise from natural inflow disturbances in the system, which are amplified at the nozzle throat. When working with dense organic vapors, even minor perturbations create sufficiently large density gradients, rendering Mach lines visible in images captured by sensitive schlieren setups. Further details of this experiment are discussed by Beltrame et al. (2021).

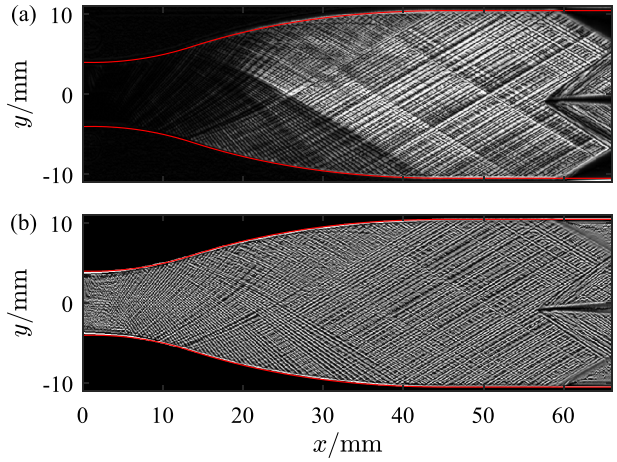

Fig. 1 **a** Raw schlieren image and **b** processed image of the supersonic flow of the dense vapor of MM through the ORCHID nozzle test section, which includes a metallic wedge at the nozzle outlet (Beltrame et al. 2021). Mach lines can be observed throughout the flow field and correspond to the characteristic lines computed to design the nozzle. Oblique shocks are generated at the leading edge of the wedge, which features a tip angle of 5°

For the purposes of this study, the raw schlieren image (Fig. 1a) is processed such as to eliminate brightness variations which, in this example, are the result of high density gradients along the streamwise direction. The procedure involves three consecutive operations on the raw image intensity matrix, I_0. First, the minimum intensity over a sliding window, $w(x, y)$, of 3×3 pixels is subtracted, that is,

$$I_1(x,y) = I_0(x,y) - \min_{x,y\in w} I_0(x,y), \tag{1}$$

thus increasing the image contrast. This operation is followed by normalization with a local average sliding window, namely,

$$I_2(x,y) = \frac{I_1(x,y)}{\overline{I_1(x,y)}_{x,y\in w}}, \tag{2}$$

thus, achieving uniform intensity. Finally, the intensity matrix is scaled by the global maximum value, which in mathematical terms gives

$$I(x,y) = \frac{I_2(x,y)}{\max\limits_{x,y\in w} I_2(x,y)}. \tag{3}$$

The components of the processed image matrix $I(x, y)$ range therefore from 0 to 1 (Fig. 1b).

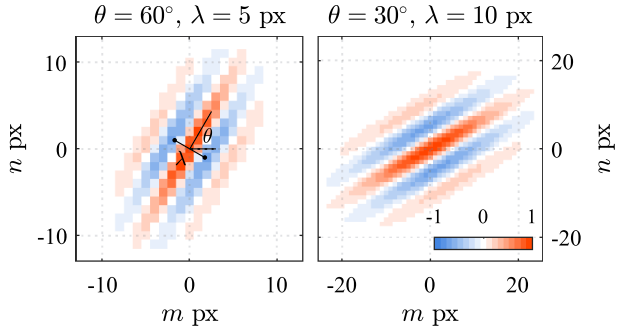

Fig. 2 Examples of the Gabor filters used to process the exemplary schlieren image of Fig. 1, obtained by varying the angle (degrees) and the wavelength (pixels per cycle). The Gaussian ellipse aspect ratio is 1:2 and the spatial frequency bandwidth is 1

3 Gabor filter methodology

A spatial, two-dimensional Gabor wavelet is constructed by modulating a sinusoid carrier with a Gaussian elliptical envelope. This family of two-dimensional Gabor functions is employed

$$g(x,y) = \cos\left(2\pi\frac{x'}{\lambda} + \phi\right)\exp\left(-\frac{x'^2 + \gamma^2 y'^2}{2\sigma^2}\right). \tag{4}$$

In Eq. (4), x' and y' are the transformed coordinates of the Gabor wavelet in the image coordinate frame (x, y), characterized by an orientation θ, i.e.,

$$x' = x\cos\theta - y\sin\theta,$$
$$y' = x\sin\theta + y\cos\theta.$$

Parameter γ is the spatial aspect ratio of the elliptical Gaussian envelope, controlling the ellipticity or anisotropy of the Gaussian envelope, hence, affecting the elongation of the filter. For the purpose of this work, γ is fixed to a value of 0.5, thus generating an elongated filter that matches closer with the Mach lines. The λ and ϕ parameters correspond to the wavelength and phase offset of the Gabor wavelet, respectively. However, for the purpose of this work, a symmetric wavelet is set, hence $\phi = 0$. Finally, σ is the standard deviation of the Gaussian envelope, estimated with

$$\sigma = \frac{\lambda}{\pi}\sqrt{\frac{\ln 2}{2}}\left(\frac{2^b + 1}{2^b - 1}\right), \tag{5}$$

where b is the linear filter's half-response spatial frequency bandwidth of $g(x, y)$ in octaves. Results in this report pertain to an arbitrarily chosen octave, i.e., the one that is obtained for $b = 1$.

With these assumptions, a family of Gabor wavelets is constructed by varying only the orientation and

wavelength parameters (θ, λ), two examples of which are shown in Fig. 2. The response, $C(x, y)$, of an image, $I(x, y)$, to each wavelet is determined by a two-dimensional convolution procedure given by

$$C_{\theta,\lambda}(x,y) = \sum_{\tau_x}\sum_{\tau_y} I(x,y)\cdot g_{\theta,\lambda}(x-\tau_x, y-\tau_y), \tag{6}$$

where τ_x and τ_y correspond to translation along x and y, respectively.

Identification of the most prominent orientation and wavelength at each pixel location of the image is performed by considering the local response map of the image to each Gabor function, i.e., the convolution coefficient defined by Eq. 6. An example of such a map is shown in Fig. 3. In this case, θ and λ are varied by steps of 1° and 0.25 px, respectively; thus, the response map is made with discrete values of C. The matrix indices (i, j) where C is maximized are first determined. The exact location of the peak is estimated by interpolation of a two-dimensional Gaussian fit, similarly to what is done to estimate the sub-pixel displacement in the cross-correlation methods utilized for particle image velocimetry (Willert and Gharib 1991). More specifically, the interpolated orientation and wavelength are shifted by $\Delta\theta$ and $\Delta\lambda$ with respect to the maximum of the discrete response map, formulated as

$$\Delta\theta = \frac{\ln C_{i-1,j} - \ln C_{i+1,j}}{2\left(\ln C_{i-1,j} - 2\ln C_{i,j} + \ln C_{i+1,j}\right)}, \tag{7}$$

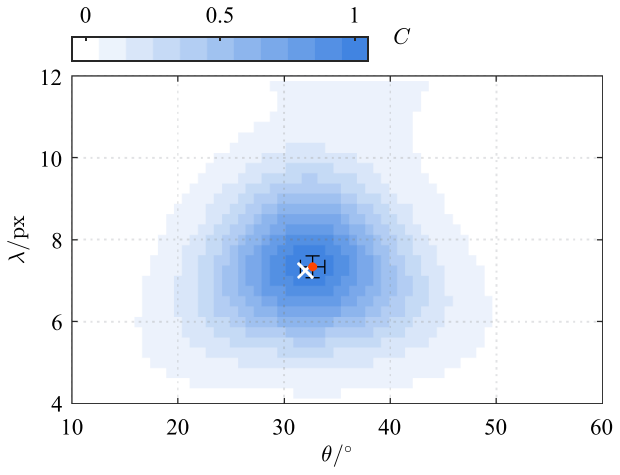

Fig. 3 Contours of the discrete response C of a single image pixel to a family of Gabor wavelets with different orientation and wavelength. The white cross indicates the location where C is maximized. The red mark identifies the location of the peak, interpolated by fitting a two-dimensional Gaussian function. Error bars visualize the standard deviations of θ and λ, determined via the joint second statistical moment (i.e., the variance)

$$\Delta\lambda = \frac{\ln C_{i,j-1} - \ln C_{i,j+1}}{2\left(\ln C_{i,j+1} - 2\ln C_{i,j} + \ln C_{i,j-1}\right)}. \tag{8}$$

To determine the uncertainty of λ and θ, the second statistical moment (i.e., the variance or σ^2) of C of each of the parameters is considered. Uncertainty of the estimated orientation and wavelength (ε_θ and ε_λ, respectively) is thus defined by the square root of the joint variance, formulated as

$$\varepsilon_\theta = \left[\sum_\theta\sum_\lambda \left(\theta-\overline{\theta}\right)^2 C(\theta,\lambda)\delta\lambda\delta\theta\right]^{0.5}, \tag{9}$$

$$\varepsilon_\lambda = \left[\sum_\theta\sum_\lambda \left(\lambda-\overline{\lambda}\right)^2 C(\theta,\lambda)\delta\lambda\delta\theta\right]^{0.5}. \tag{10}$$

In Eqs. (9) and (10), the mean values $\overline{\theta}$ and $\overline{\lambda}$ correspond to the peak value obtained by interpolation via Gaussian fitting.

In the exemplary convolution map shown in Fig. 3, the maximum of C and the peak resulting from Gaussian fitting do not match, owing to the non-perfect Gaussian distribution of the orientation and wavelength data. A better estimate of the peak can be obtained by employing the two-dimensional Gaussian regression method (Nobach and Honkanen 2005). In the case of this dataset, the difference between the two estimates is small (< 2%) and falls within the evaluated uncertainty, bounded by the error bars corresponding to the standard deviation of λ and θ (Fig. 3).

4 Radon transform methodology

In the context of this work, the objective of the Radon transformation is to project the integral of image intensity on a line normal to a projection angle θ. This operation may be repeated for a range of projection angles to obtain a sinogram, i.e., a map of intensity projections for all projection angles. The projection angle at which the sinogram is maximized, therefore, corresponds to the orientation angle of the most dominant flow feature.

The pre-processed image, I, is subdivided in interrogation windows, as shown in Fig. 4a. The diameter of the window should be selected such that it encompasses features of interest, in this case a few Mach lines. To improve spatial resolution, overlap can be applied between interrogation windows in both the x and the y direction. In order to ensure an equal radial integration length for all projection angles, a two-dimensional top-hat filter is applied to each interrogation window, resulting in the circular window highlighted in the figure.

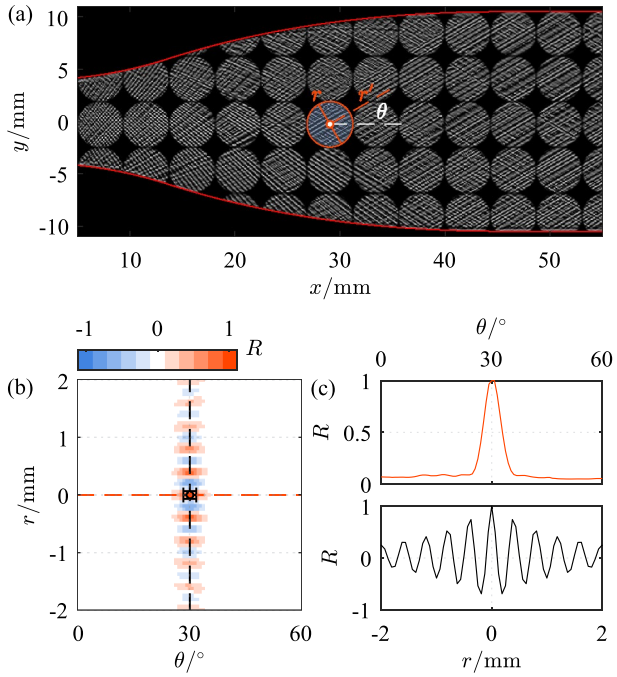

Fig. 4 **a** Subdivision of the processed schlieren image into interrogation windows. A two-dimensional top-hat filter is applied to each interrogation window. In this example, interrogation window sizes feature a diameter of 4.3 mm and 0 % overlap. **b** Normalized Radon transform amplitude (R) of the auto correlation of the interrogation window marked in **a**. The horizontal and vertical error bar related to the location of maximum intensity visualize the uncertainty of θ and λ, respectively. **c** Top chart: R along the red dashed line in **b**. bottom chart: R along the black dashed line in **b**

To determine the Mach line orientation, first a polar coordinate system is defined with the origin at the center of each interrogation window, see Fig. 4a. The sinogram of each interrogation window is subsequently calculated by applying the integral Radon transform to the autocorrelation of the interrogation window intensity $I^\star$ for a range of projection angles θ, that is

$$R(\theta, r) = \int_{-\infty}^{\infty} I^\star(r\cos\theta - r'\sin\theta, r\sin\theta + r'\cos\theta)\mathrm{d}r', \quad (11)$$

where r' and r are the radial coordinate along a line parallel and normal to the projection angle, respectively. Note that autocorrelation is preferred in order to disregard random noise in the window while maintaining strong features. The resulting sinogram is shown in Fig. 4b which, for this interrogation window, features a maximum at $\theta = 30.8°$. The chart at the top of Fig. 4c shows that R is characterized by a Gaussian distribution along the range of orientations; hence, it is possible to interpolate the peak orientation angle following the same method described in Sect. 3 (Eq. 7), albeit limited to one dimension. As a result, due to the repetitive pattern of the Mach lines, the amplitude of the sinogram exhibits wave-like trend along the radial direction, cf. the bottom chart of Fig. 4c. This enables the estimation of the distance between Mach lines using standard signal processing techniques such as the spatial Fourier transform or wavelet analysis. Given the relatively short signal length, in this study we chose to employ 1D wavelet analysis, specifically the Morlet wavelet (Daubechies 1992). A response map of normalized wavelet coefficients, C_w is obtained with r as the abscissa and λ as the ordinate. The response map is similar to that displayed in Fig. 3. The exact wavelength is subsequently determined through a 1D Gaussian fit limited to the vicinity of the maximum value of C_w, according to Eq. 8.

Similar to the Gabor filtering methodology, uncertainties on the orientation and wavelength of Mach lines are estimated via the second statistical moment of R and C_w, respectively, formulated as

$$\varepsilon_\theta = \left[\sum_\theta \left(\theta - \bar{\theta}\right)^2 R(\theta)\delta\theta\right]^{0.5}, \quad (12)$$

and

$$\varepsilon_\lambda = \left[\sum_\lambda \left(\lambda - \bar{\lambda}\right)^2 C_\mathrm{w}(\lambda)\delta\lambda\right]^{0.5}. \quad (13)$$

All the results pertaining to the application of the Radon methodology presented in Sect. 5 are obtained with an interrogation window with a diameter of 3.5 mm (56 px) and 85% overlap, achieving comparable spatial resolution as with the Gabor filter approach.

5 Results

Figure 5a, b visualizes the orientation of the Mach lines displayed in the schlieren photograph of Fig. 1, computed via the Gabor filtering and Radon transform methodologies, respectively. The figures also show that the orientations obtained with the two post-processing procedures are in excellent agreement. Consistently with the pattern that can be observed in the processed raw image (Fig. 1b), the Mach line angle gradually decreases along the streamwise direction, starting at approximately 55° near the throat down to 31° toward the nozzle exit. This variation of the Mach angle complies with the features of the paradigmatic supersonic flow expanding through a nozzle, which can be partitioned into three distinct zones: the kernel, the reflex, and the uniform regions, as outlined by Anand et al. (2019). In the kernel region, the flow accelerates and reaches the design Mach number, while in the reflex region the expanding flow

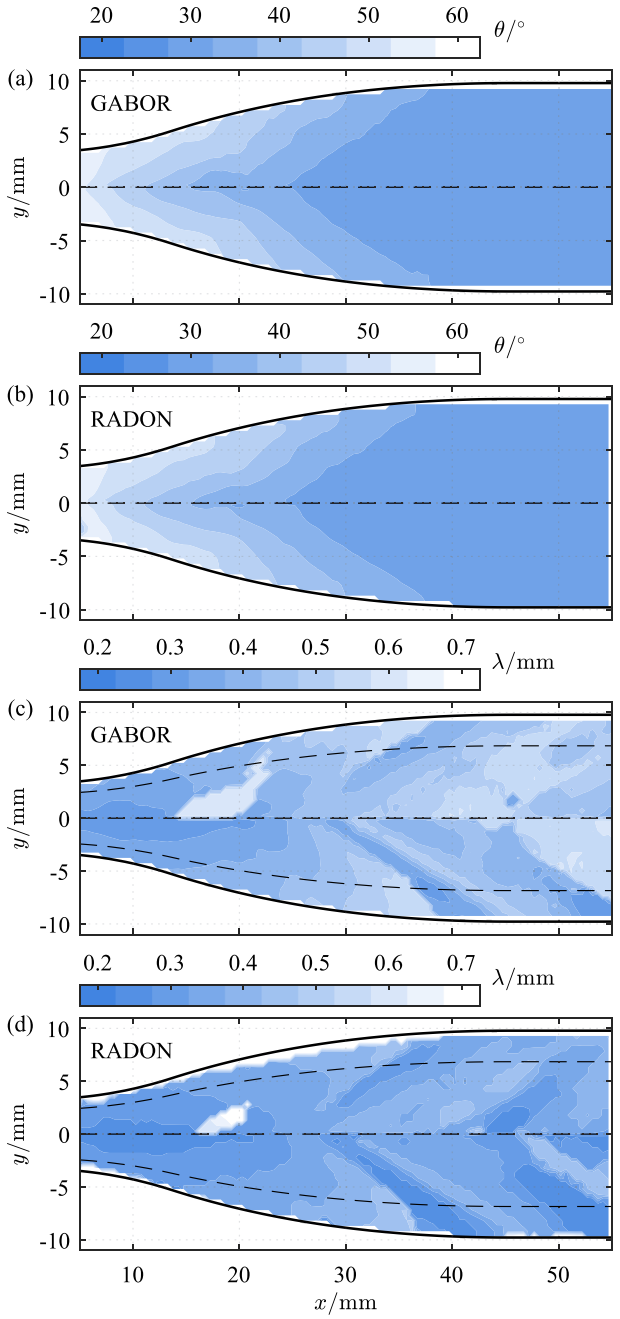

Fig. 5 Orientation of the Mach lines displayed in the schlieren image of Fig. 1a calculated with the Gabor (**a**) and Radon (**b**) methodology. Mach line wavelength calculated with the Gabor (**c**) and Radon (**d**) methodology. Dashed lines correspond to values of −0.7, 0 and 0.7 of the nozzle geometry y coordinate

is appropriately deviated so as to achieve a uniform velocity profile at the nozzle exit.

In addition to the Mach line orientation, in case such need arises, the proposed methodologies are capable of estimating the distance between features in schlieren images such as the Mach lines in figure 1a. More specifically, the identified wavelengths (px) estimated with the proposed methodologies are multiplied with the image calibration (mm/px), to obtain the distance of the Mach lines within the field of view. The estimated fields for this example are shown in Fig. 5c (Gabor) and d (Radon), whereby distances between Mach lines range from 0.3 mm near the throat to 0.5 mm in the uniform flow region. Also in this case, the agreement between the results obtained by applying the two methodologies is remarkable. In addition, with reference to Fig. 1b, it can be observed that both techniques can be used to detect the local variations of the Mach lines that develop along the characteristic lines of the nozzle design in the conditions at hand. As expected, therefore, the Mach line density does not affect the estimated value of the Mach line orientation.

Using the Mach line orientation as a reference, it is possible to estimate the Mach number of the flow along the nozzle. More specifically, the Mach number can be calculated as

$$M = \frac{1}{\sin\theta}, \tag{14}$$

assuming flow symmetry with respect to the nozzle centerline $y = 0$. Figure 6 allows to perform a comparative analysis by juxtaposing the orientation of Mach lines and the corresponding Mach numbers. These estimations are obtained utilizing the Gabor and Radon methodologies, the Hough transform line detection technique, and the results of an Euler flow simulation reported by Head et al. (2023). The uncertainties on the average of all the values are also provided, propagated through to the calculation of the Mach number. All the calculated values are in very good agreement. In comparison with values calculated with the Hough transform technique, values computed with the Gabor and Radon methodologies are characterized by better spatial resolution. This advantage stems from these methods being independent from edge-based computations (i.e., on the number of Mach lines), contrary to the Hough transform approach. In addition, the robustness of the proposed methodologies, owing to feature detection over an area, results in lower uncertainties in the vicinity of the throat (3%) where Mach lines are more regular. However, for the remainder of the field of view the uncertainty associated with values calculated with all the mentioned methods is comparable (5%).

Figure 5 allows to perform a more detailed comparison of the two methodologies regarding the identification of the distance between Mach lines. The figure shows the estimated distances for selected values of the y coordinate with respect to the nozzle geometry (y_n), which are reported as dashed lines in Fig. 5. More specifically, Fig. 7 displays wavelengths for values of y_n equal to −0.7, 0, and 0.7 of y_n along with the associated uncertainties. Overall, there is once again very good agreement between the values predicted with the two methods. However, results obtained with Gabor filtering are affected by lower uncertainties (12.5%) compared to those

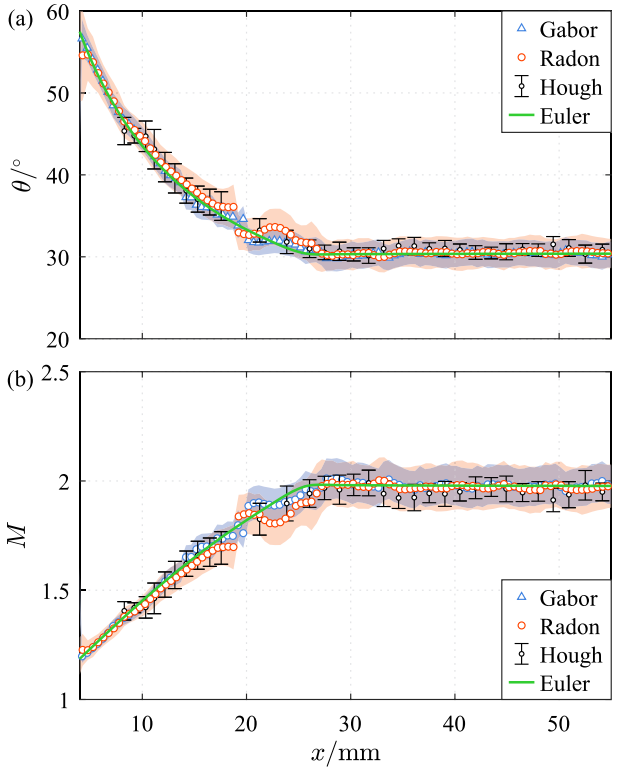

Fig. 6 With reference to the schlieren image of Fig. 1a: **a** Mach line orientation and **b** Mach number at the centerline. Comparison of results obtained with Gabor filtering, Radon transform, Hough transform (Head et al. 2023), and an Euler numerical simulation of the flow. The shaded bands provide the visualization of the uncertainty of the values calculated with the Gabor and Radon methodologies. The values calculated with the Hough transform are reported with the respective error bars

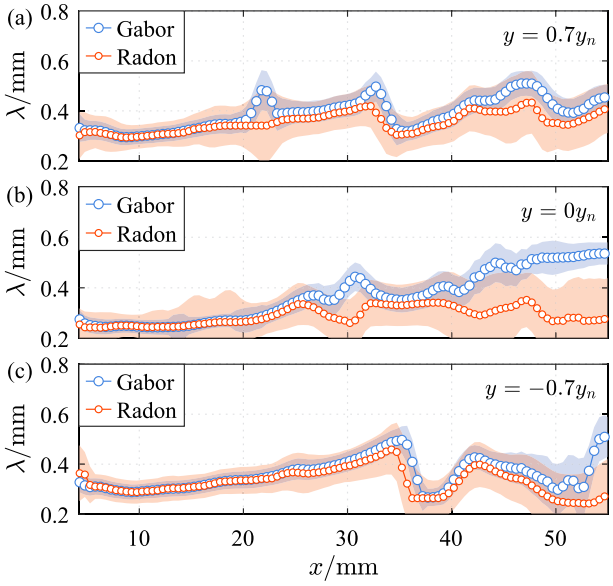

Fig. 7 Wavelength of Mach lines estimated with the Gabor filter and Radon transform methodologies for at (**a**) −0.7, (**b**) 0, and (**c**) 0.7 of the nozzle y coordinate (corresponding to the dashed lines displayed in Fig. 5)

calculated with the Radon transform m(25.3%). This difference can be explained by considering that uncertainties of the values computed with the Gabor filtering method are estimated jointly for orientation and wavelength, whereas the Radon transform method relies solely on the wavelength parameter and only for a short signal due the interrogation window. An important remark is that although these uncertainties are rather large, they correspond to 0.8 px and 1.4 px for the Gabor filtering and Radon transform methodologies, respectively. Therefore, these uncertainties are approximately of the same magnitude of the resolution limit of the camera and thus are deemed admissible.

Finally, the performance of the two methodologies for the estimation of the local Mach number is further evaluated by considering the flow region surrounding the wedge. Figure 8a shows a closeup of the schlieren image of this region. Hereby, due to the particularities or organic vapor flows, images capture clearly both Mach lines emanating from the nozzle as well as oblique shock waves stemming from the leading edge of the wedge. It can be

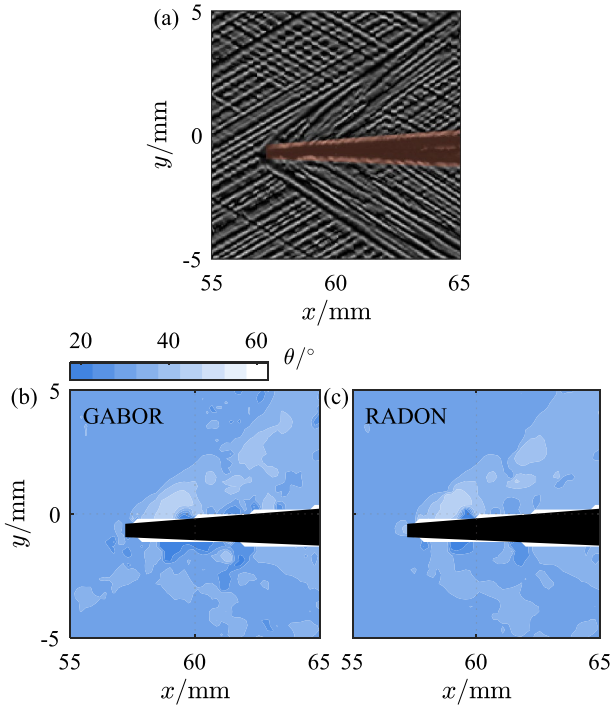

Fig. 8 Features in the flow region close to the wedge protruding in the uniform region of the nozzle (see Fig. 1) (**a**) schlieren image and **b** and **c** Mach line orientation field as estimated via the Gabor and Radon methodologies, respectively

observed that the positioning of the wedge is not aligned to the axis of the nozzle and that it is tilted slightly downward. This misalignment causes a non-symmetrical pressure gradient and, thus, a notable difference between the angle of the shock wave atop the wedge if compared to the angle of the Mach lines distributed over the rest of the uniform region. Figure 8b, c demonstrates that both post-processing methods are able to capture this compressible flow features, underscoring the suitability of such techniques for discerning Mach line orientation even in the case of very complex flow fields.

6 Concluding remarks

In this study, we explore characterization of features in compressible flows, specifically Mach lines and shock waves, by employing Gabor filtering and Radon transform techniques. To illustrate the potential of this approach, the methodology is applied to an experimental test case involving a dense organic vapor flow within a supersonic nozzle. At the nozzle outlet, a wedge is positioned, generating oblique shocks. The computed Mach line orientation and Mach number are compared with estimations obtained in past studies using the Hough transform methodology and numerical Euler simulations. Remarkably, for the same flow conditions, the results demonstrate excellent agreement. A comparative analysis highlights several advantages of the proposed methodologies. First, in contrast to the Hough transform technique, Mach line orientations are estimated in the entirety of the field of view, accompanied by estimations of Mach line wavelength. Second, both approaches offer superior spatial resolution, with uncertainties which are on par with the Hough transform technique. Lastly, considering the coexistence of Mach waves and shock waves in the vicinity of the wedge, the results emphasize the robustness of the proposed techniques in accurately identifying superimposed flow features.

Author contributions T. M. and A. J. wrote the main manuscript text and prepared all figures. P. C. contributed the abstract and conclusions and performed a first peer review. All authors reviewed the manuscript.

Data availability The data supporting the findings of this study can be made available upon reasonable request.

Declarations

Conflict of interest Not applicable. The authors declare no conflict of interest.

Ethical approval Not applicable.

References

Anand N, Vitale S, Pini M, Otero GJ, Pecnik R (2019) Design methodology for suoersonic radial vanes operating in nonideal flow conditions. J Eng Gas Turb Power 141(2):022601

Arrospide J, Salgado L (2013) Log-gabor filters for image-based vehicle verification. IEEE Trans Image Process 22:2286–2295

Beltrame F, Head AJ, De Servi C, Pini M, Schrijer F, Colonna P (2021) First Experiments and Commissioning of the ORCHID Nozzle Test Section. ERCOFTAC Ser 28:169–178

Beylkin G (1987) Discrete radon transform. IEEE Trans Acoust Speech Signal Process. 35(2)

Canchero A, Tinney CE, Murray N, Ruf JH (2016) Acoustic imaging of clustered rocket nozzles undergoing end effects. AIAA J 54(12):3778–3786

D'Aguanno A, Camps Pons C, Shrijer FFJ, van Oudheusden BW (2022) Experimental study of the effect of wing sweep on transonic buffet. In: AIAA SciTech Forum (San Diego, CA & Virtual)

Daubechies I (1992) Ten Lectures on Wavelets, CBMS-NSF regional conference series in applied mathematics, vol 61. SIAM

Duda RO, Hart PE (1972) Use of the hough transformation to detect lines and curves in pictures. Commun ACM 15(1):11–15

Field DJ, Hayes A, Hess RF (1993) Contour integration by the human visual system: evidence for a local "association field''. Vision Res 33:173–193

Guardone A, Colonna P, Pini M, Spinelli A (2024) Nonideal compressible fluid dynamics of dense vapors and supercritical fluids. Annu Rev Fluid Mech 56:241–269. https://doi.org/10.1146/annurev-fluid-120720-033342

Head AJ, Michelis T, Beltrame F, Fuentes-Monjas B, Casato E, de Servi C, Colonna P (2023) Mach number estimation and pressure profile measurements of expanding dense organic vapors. In: Proceedings of the 4th international seminar on non-ideal compressible fluid dynamics for propulsion and power,ERCOFTAC, Vol. 29. Springer Nature Switzerland, pp. 229–238

Head AJ (2021) Novel experiments for the investigation of non-ideal compressible fluid dynamics: the ORCHID and first results of optical measurements. Ph.D. thesis (Delft University of Technology)

Jain AK, Farrokhnia F (1991) Unsupervised texture segmentation using Gabor filters. Pattern Recogn 24(12):1167–1186

Lo R-C, Tsai W-H (1995) Gray-scale Hough transform for thick line detection in gray-scale images. Pattern Recogn 28(5):647–661

Michelis T, Head AJ, Majer M, Colonna P, De Servi C (2024) Assessment of particle image velocimetry applied to high-speed organic vapor flows. Exp Fluids 65(6):1–9

Murray NE, Lyons GW (2016) On the convection velocity of source events related to supersonic jet crackle. J Fluid Mech 793:477–503

Nobach H, Honkanen M (2005) Two-dimensional Gaussian regression for sub-pixel displacement estimation in particle image velocimetry or particle position estimation in particle tracking velocimetry. Exp Fluids 38:511–515

Randen T, Husøy JH (1999) Filtering for texture classification: a comparative study. IEEE Trans Pattern Anal Mach Intell 21(4):291–310

Spinelli A, Cammi G, Gallarini S, Zocca M, Cozzi F, Gaetani P, Dossena V, Guardone A (2018) Experimental evidence of non-ideal compressible effects in expanding flow of a high molecular complexity vapor. Exp Fluids 59:126

Tam KC, Samarasekara S, Sauer F (1998) Exact cone beam CT with a spiral scan. Phys Med Biol 43:1015–1024

Willert CE, Gharib M (1991) Digital particle image velocimetry. Exp Fluids 10:181–193